Meteoritics & Planetary Science 36, 531–548 (2001)
Available online at http://www.uark.edu/meteor

Mineralogy and petrology of the Dar al Gani 476 martian meteorite: Implications for its cooling history and relationship to other shergottites

TAKASHI MIKOUCHI[1,2]*, MASAMICHI MIYAMOTO[2] AND GORDON A. MCKAY[1]

[1]Mail Code SN2, Planetary Science Branch, NASA Johnson Space Center, Houston, Texas 77058, USA
[2]Department of Earth and Planetary Science, Graduate School of Science, University of Tokyo, 7-3-1 Hongo, Bunkyo-ku, Tokyo 113-0033, Japan
*Correspondence author's e-mail address: mikouchi@eps.s.u-tokyo.ac.jp

(Received 1999 December 13; accepted in revised form 2000 December 20)

Abstract–Dar al Gani 476, the 13th martian meteorite, was recovered from the Sahara in 1998. It is a basaltic shergottitic rock composed of olivine megacrysts reaching 5 mm (24 vol%) set in a fine-grained groundmass of pyroxene (59 vol%) and maskelynitized plagioclase (12 vol%) with minor amounts of accessory phases (spinel, merrillite, ilmenite). Dar al Gani 476 is similar to lithology A of Elephant Moraine A79001 (EETA79001) in petrography and mineralogy, but is distinct in several aspects. Low-Ca pyroxenes in the Dar al Gani 476 groundmass are more magnesian ($En_{76}Fs_{21}Wo_3$~$En_{58}Fs_{30}Wo_{12}$) than those in lithology A of EETA79001 ($En_{73}Fs_{22}Wo_5$~$En_{45}Fs_{43}Wo_{12}$), rather similar to pyroxenes in lherzolitic martian meteorites ($En_{76}Fs_{21}Wo_3$~$En_{63}Fs_{22}Wo_{15}$). Dar al Gani 476 olivine is less magnesian and shows a narrower compositional range (Fo_{76-58}) than EETA79001 olivine (Fo_{81-53}), and is also similar to olivines in lherzolitic martian meteorites (Fo_{74-65}). The orthopyroxene-olivine-chromite xenolith typical in the lithology A of EETA79001 is absent in Dar al Gani 476. It seems that Dar al Gani 476 crystallized from a slightly more primitive mafic magma than lithology A of EETA79001 and several phases (olivine, pyroxene, chromite, and ilmenite) in Dar al Gani 476 may have petrogenetic similarities to those of lherzolitic martian meteorites. Olivine megacrysts in Dar al Gani 476 are in disequilibrium with the bulk composition. The presence of fractured olivine grains in which the most Mg-rich parts are in contact with the groundmass suggests that little diffusive modification of original olivine compositions occurred during cooling. This observation enabled us to estimate the cooling rates of Dar al Gani 476 and EETA79001 olivines, giving similar cooling rates of 0.03–3 °C/h for Dar al Gani 476 and 0.05–5 °C/h for EETA79001. This suggests that they were cooled near the surface (burial depth shallower than about 3 m at most), probably in lava flows during crystallization of groundmass. As is proposed for lithology A of EETA79001, it may be possible to consider that Dar al Gani 476 has an impact melt origin, a mixture of martian lherzolite and other martian rock (Queen Alexandra Range 94201, nakhlites?).

INTRODUCTION

Dar al Gani 476 was recovered from the Sahara in May 1998 and classified as a basaltic shergottite (Zipfel, 1998), the largest group of martian meteorites (*e.g.*, McSween, 1994). Dar al Gani 476 is the 13th martian meteorite and is one rock fragment originally weighing 2015 g. The number of martian meteorites is constantly growing because of the recent recovery of thousands of meteorites from both Antarctica and African deserts. The 14th martian meteorite, Dar al Gani 489 from the Sahara, was also announced to the meteoritical community, and pairing with Dar al Gani 476 is plausibly considered (Grossman, 1999; Folco *et al.*, 1999, 2000). After the discovery of Dar al Gani 489, two additional shergottites (Dar al Gani 670 and Dar al Gani 735) were discovered from the same region and they were also likely to be the paired meteorites with Dar al Gani 476/489 (Folco and Franchi, 2000; Grossman, 2000).

Preliminary reports indicate that Dar al Gani 476 is similar to lithology A of Elephant Moraine A79001 (EETA79001) in petrography (Mikouchi, 1999; Zipfel *et al.*, 1999). EETA79001 is known to contain two different igneous lithologies designated A and B, separated by a linear contact, and also contains pockets and veinlets of dark glass, labeled lithology C (Reid and Score, 1981). EETA79001 is the first meteorite found to contain a geological contact between two lithologies in the same meteorite sample. There have been a large number of studies investigating noble gas characteristics of this meteorite due to isotopic compositions matching those of the martian atmosphere as

Prelude preprint MS#4265

measured by the *Viking* lander (*e.g.*, Bogard and Johnson, 1983; Becker and Pepin, 1984; Ott and Begemann, 1985; Wiens, 1988; Bogard and Garrison, 1998), as well as its mineralogical and petrological characteristics (Steele and Smith, 1982; McSween and Jarosewich, 1983; Jones, 1986; Wadhwa *et al.*, 1994; Mittlefehldt *et al.*, 1999; Mikouchi *et al.*, 1999b). Nevertheless, discovery of Dar al Gani 476 invites comparison with EETA79001 and thus provides a good opportunity to reevaluate the petrogenesis of the basaltic shergottites. In spite of close textural similarities between Dar al Gani 476 and lithology A of EETA79001, isotopic and trace element studies instead suggest a closer genetic relationship of Dar al Gani 476 to Queen Alexandra Range (QUE) 94201, nakhlites and Chassigny (Jagoutz *et al.*, 1999; Zipfel *et al.*, 1999, 2000; Wadhwa *et al.*, 1999). Furthermore, the highly mafic composition of Dar al Gani 476 implies a closer petrological relationship to lherzolitic groups than EETA79001 does (Mikouchi, 1999; Zipfel *et al.*, 2000). Thus, discovery of Dar al Gani 476 may help to clarify the petrogenetic relationship of all Shergotty-Nakhla-Chassigny (SNC) meteorites, especially relationships between the basaltic and lherzolitic martian meteorites, and may thus provide important clues to their formation on Mars.

In this paper we present the results of mineralogical investigations of Dar al Gani 476 based upon petrographic observations and electron microprobe analyses of a polished section. At the same time we also analyzed lithology A of EETA79001 and Yamato-793605 lherzolitic martian meteorite (Y-793605) so that we could directly compare their mineral compositions in order to better understand their petrogenetic relationships.

SAMPLES AND ANALYTICAL TECHNIQUE

We analyzed polished sections of Dar al Gani 476 and lithology A of EETA79001. The University Museum, University of Tokyo and Max-Planck-Institut für Chemie (Dr. J. Zipfel) supplied small rock chips of Dar al Gani 476 and a polished section was prepared. The size of the section is about 10 × 5 mm. A polished thin section of lithology A of EETA79001 (EETA79001,443) was supplied by the Meteorite Working Group (NASA Johnson Space Center). For a comparative study we also analyzed Y-793605 lherzolitic martian meteorite supplied by National Institute of Polar Research (Tokyo, Japan). Backscattered electron (BSE) images were taken with JEOL JXA840 and Hitachi S-4500 scanning electron microscopes with energy dispersive spectrometers (EDS) (Department of Earth and Planetary Science, University of Tokyo). Elemental distribution maps were acquired by a JEOL JXA 8900L electron microprobe (Department of Earth and Planetary Science, University of Tokyo). Accelerating voltage was 15 kV, and the beam current was 60–120 nA. Quantitative wavelength dispersive analyses were performed by a JEOL Superprobe 733 electron microprobe (Ocean Research Institute, University of Tokyo), a JEOL JCM 733 mk II microprobe (Department of Earth and Planetary Science, University of Tokyo), and Cameca SX100 electron microprobe (NASA Johnson Space Center). Quantitative analyses of most phases were obtained at 15 kV accelerating voltage with a beam current of 12–20 nA on a Faraday cage. Because plagioclase glass (maskelynite) shows high mobility of Na under the electron beam, we employed very gentle conditions for plagioclase analysis (defocused beam of ~10 μm in diameter and probe current of 8 nA) to minimize volatile loss during analysis.

RESULTS

Macroscopic Observation

First, we report a macroscopic observation of Dar al Gani 476 because we had a chance to take a brief look at the main mass at The Tokyo Mineral Show in December 1998.

Dar al Gani 476 is a greenish-brown rock without typical fusion crust. The overall color is similar to those of lherzolitic martian meteorites (Allan Hills (ALH) 77005, Lewis Cliff (LEW) 88516 and Yamato (Y-793605) (*e.g.*, Yanai and Kojima, 1981) rather than EETA79001 which is grayish white in color (*e.g.*, Meyer, 1998). Dar al Gani 476 is fairly weathered probably due to the severe climate of the desert. The fusion crust may have been removed by weathering during residence in the desert. Many large olivine grains (up to 5–6 mm long) were observed on both the weathered surface and the sawn surface (Fig. 1). Olivines are slightly jutting out from the weathered surface probably because olivine is more resistant against weathering or because of its larger grain size than other minerals (pyroxene and plagioclase). In large individual olivine crystals, we could observe a detailed inner texture and color variation. These olivines usually have brownish orange cores with black rims, indicating chemical zoning (Fig. 1). In some areas, olivine grains appear to have a preferred orientation of their longer dimensions. The matrix is dark greenish and it is difficult to identify individual mineral grains because of the fine-grained texture. However, its color suggests the presence of abundant pyroxenes.

On the sawn surface, we observed white material along fractures (Fig. 1). This texture hints that the white mineral is a weathering product (carbonate or sulfate) if we consider that Dar al Gani 476 was recovered from the hot and dry desert. Large olivine grains with visible zoned colors are preserved even within this white material (Fig. 1). Olivine is known to be easily weathered by aqueous alteration (*e.g.*, Smith *et al.*, 1987). Therefore, the preservation of zoned olivine may suggest that this white material precipitated very quickly before olivine could be affected by weathering. The terrestrial age of Dar al Gani 476 is estimated to be about 85 ± 50 ka (Nishiizumi *et al.*, 1999). Shock melt veins were not recognized on the sawn surface although they are reported to be abundant (Zipfel *et al.*, 2000; Greshake and Stöffler, 1999).

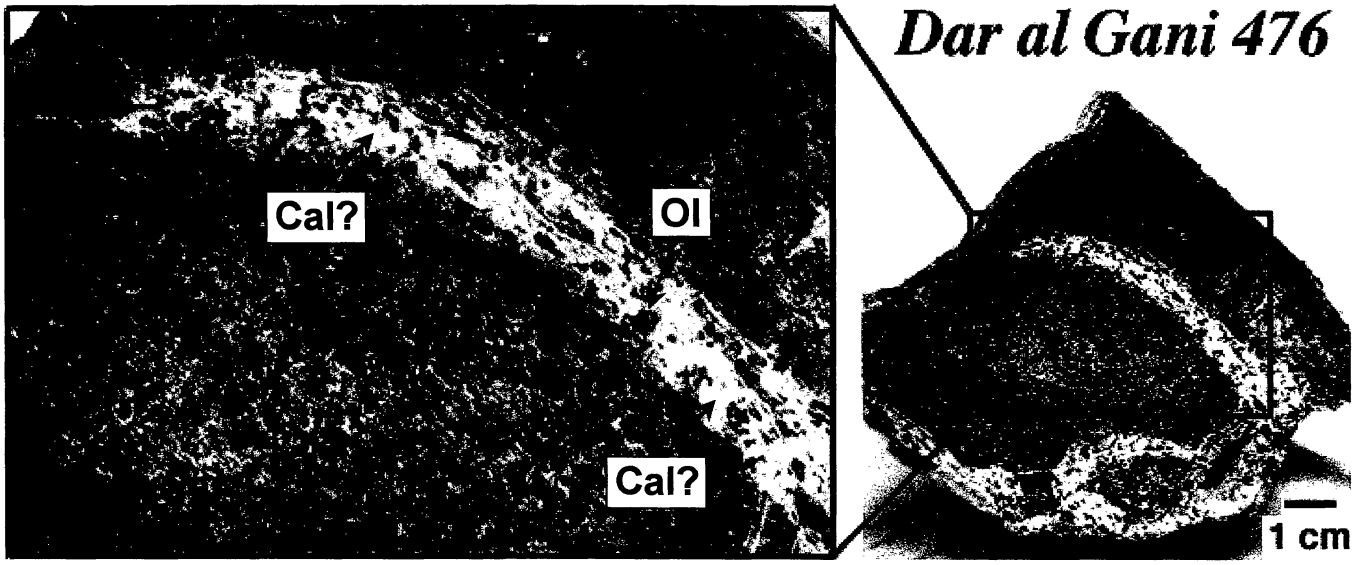

FIG. 1. Sawn surface of the Dar al Gani 476 main mass and an enlarged view. Note that a white lithology prevails along the fractures. Olivine cores and rims are visible even within this white lithology. Abbreviations: Ol = olivine, Cal = calcite.

Petrography

The polished section of Dar al Gani 476 (~10 × 5 mm) shows a basaltic porphyritic texture principally composed of pyroxene, olivine and plagioclase glass (Fig. 2). The modal abundance of minerals as estimated by a combination of several x-ray maps gives 59% pyroxene, 24% olivine, 12% plagioclase, 2% Ca carbonate, 1% spinel, 1% merrillite, and 1% others. Zipfel *et al.* (2000) also reported similar mineral modes although their sample is slightly more abundant in plagioclase and poorer in olivine.

Olivine is typically present as large single or compound crystals (reaching up to 4 mm long) set in a fine-grained groundmass mainly composed of lathy pyroxene and interstitial plagioclase glass (Fig. 2). Olivine grains are usually subhedral, but large near-euhedral crystals are sometimes observed. Small anhedral grains are also present. The extremely large size of olivine grains relative to the surrounding groundmass suggests a xenocrystic origin of these grains (Mikouchi, 1999; Mikouchi *et al.*, 1999a; Zipfel, 1999), but their euhedral to subhedral forms hint at a phenocrystic origin directly crystallized from the bulk melt (Zipfel *et al.*, 2000). Olivines are sometimes embayed by the groundmass minerals, suggesting reaction with the groundmass magma. Olivine usually contains rounded magmatic inclusions (up to 100 μm across). Fractures in olivines are sometimes filled with Ca carbonate that is probably of terrestrial origin.

Pyroxenes occur as euhedral to subhedral laths typically a few hundred microns in size. The overall texture constituted by olivine megacrysts and pyroxene laths appears to have a preferred alignment of grains. Plagioclase is anhedral and interstitial to pyroxene. As is "maskelynitized" plagioclase in the other shergottitic martian meteorites, plagioclase in Dar al Gani 476 is an isotropic glass and radiation cracks into the surrounding phases develop (Chen and El Goresy, 2000). Average grain size of the groundmass phases is about 0.1 mm long. Minor phases are chromian spinel, merrillite, Fe sulfide, ilmenite and Ca carbonates. Spinels are up to 200 μm in size and scattered within the sample. Merrillite (~100 μm long) is normally associated with Na-rich plagioclase. Magmatic inclusions within olivine are mainly composed of Al-Ti-rich pyroxene and feldspathic glass.

Almost all the present phases show chemical zoning. Although olivine shows a systematic core-to-rim zoning (although the core is not always located near the center of the grain), zoning features of some pyroxenes are rather irregular (Fig. 3). The smaller olivine grains are usually more ferroan than the larger grains and they are homogeneous.

Mineral Chemistry

Representative mineral compositions of major and minor phases in the Dar al Gani 476 are summarized in Table 1.

Olivine–Dar al Gani 476 olivine shows coherent chemical zoning from the Fo_{76} core to the Fo_{58} rim (Fig. 4). The most magnesian composition is nearly identical to that reported by Zipfel *et al.* (2000). This probably means that Fo_{76} is really the most magnesian composition of Dar al Gani 476 olivine. Manganese oxide (MnO) is correlated with FeO and is zoned from 0.4 to 0.8 wt% (Fig. 4). The FeO/MnO ratio is about 50 (by weight), which is typical of martian samples. Calcium oxide (CaO) is generally constant (0.2–0.3 wt%), but some grains

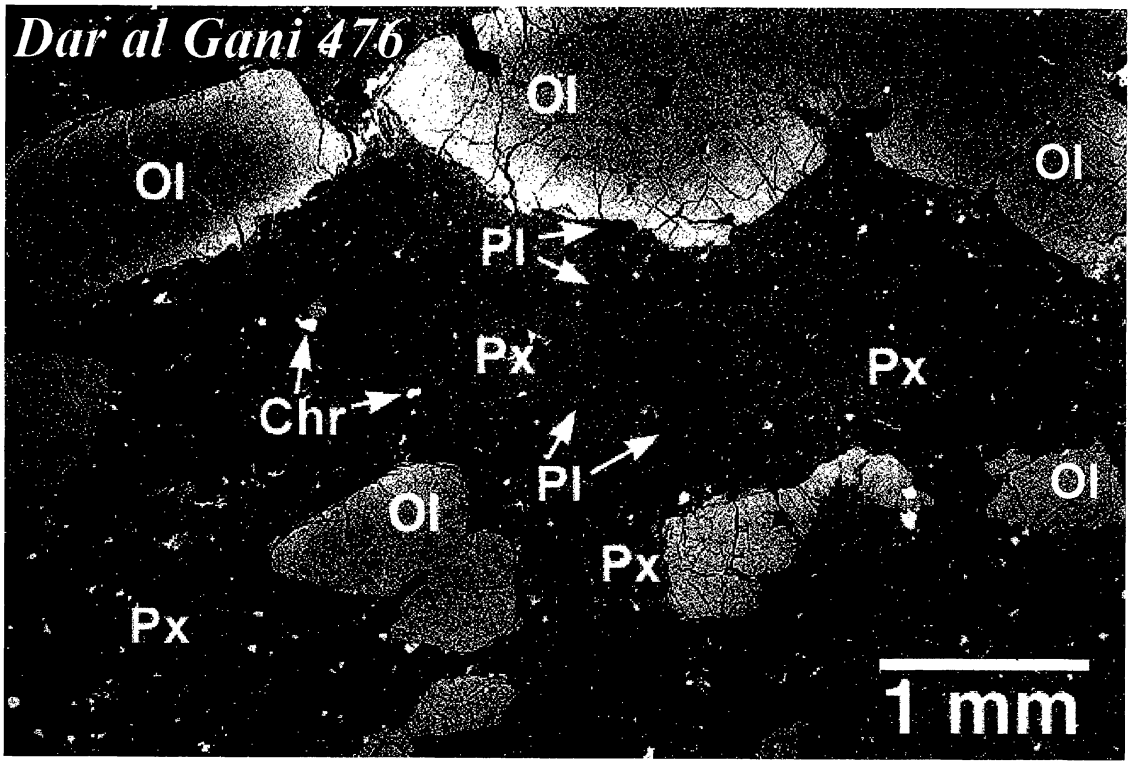

FIG. 2. Backscattered electron image of Dar al Gani 476 showing a porphyritic texture composed of olivine megacrysts and the pyroxene-plagioclase groundmass. Note that groundmass appear to fill embayments in the megacrysts. Abbreviations: Ol = olivine, Px = pyroxene, Pl = plagioclase glass, Chr = chromite.

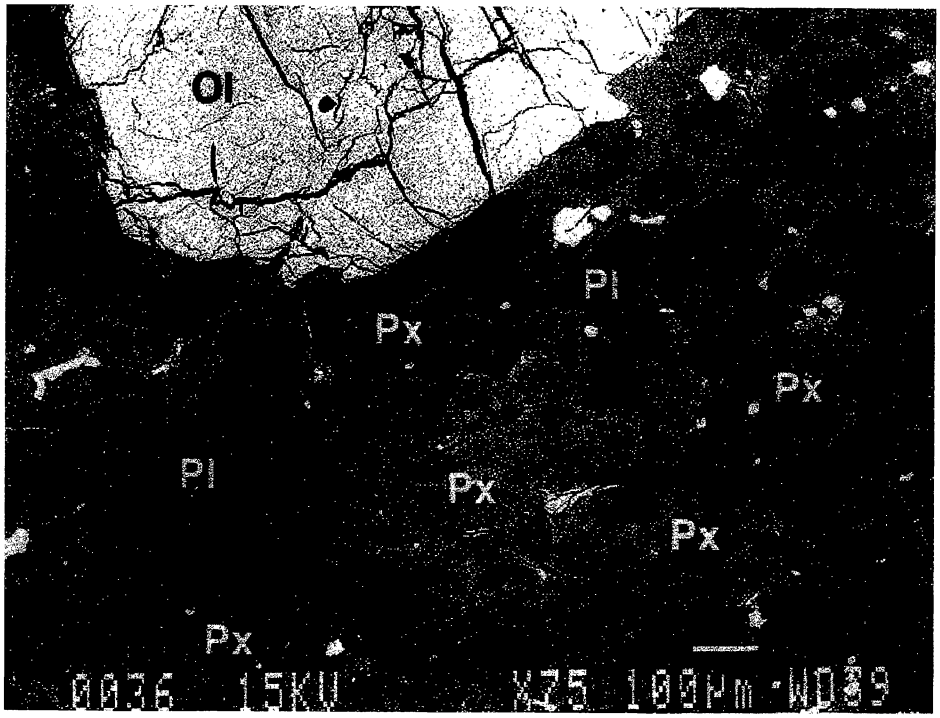

FIG. 3. Backscattered electron image of the Dar al Gani 476 groundmass near the olivine megacryst. The groundmass consists of euhedral-subhedral pyroxenes and lesser amounts of interstitial shocked plagioclase glass. Note that pyroxene shows a complicated chemical zoning texture. Abbreviations: Px = pyroxene, Ol = olivine, Pl = plagioclase, Chr = chromite.

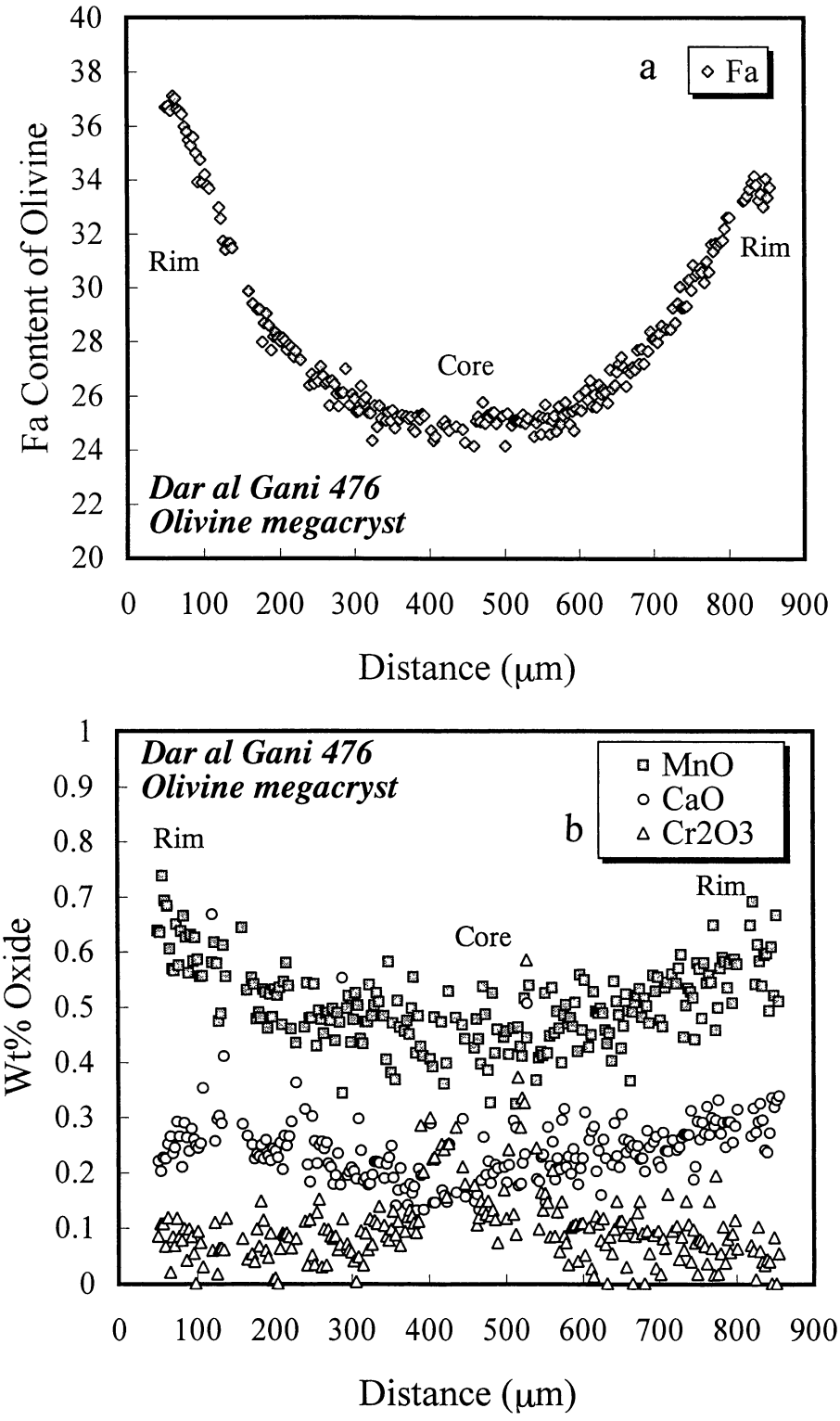

FIG. 4. Major and minor element zoning profiles of a Dar al Gani 476 olivine megacryst. (a) Fa zoning profile. Note the nice systematic pattern. (b) MnO, CaO and Cr_2O_3 zoning profiles.

TABLE 1. Representative chemical compositions of major and minor phases in Dar al Gani 476.

	1	2	3	4	5	6	7	8	9	10	11	12	13	14
SiO_2	56.12	52.65	52.34	38.03	35.99	52.35	58.63	0.11	0.02	0.14	0.06	46.39	64.91	25.20
TiO_2	0.03	0.27	0.55	–	0.06	–	0.17	5.90	20.50	–	54.10	2.08	1.18	0.06
Al_2O_3	0.46	1.16	1.80	0.04	–	30.05	26.30	6.69	3.85	0.02	0.05	10.49	15.84	2.02
FeO	12.50	18.89	11.34	22.48	35.18	0.54	0.51	33.62	46.35	1.22	38.92	9.26	3.37	44.75
MnO	0.42	0.65	0.48	0.49	0.66	0.04	–	0.33	0.64	0.01	0.70	0.32	0.17	0.81
MgO	29.03	20.19	15.94	38.13	28.28	0.24	0.15	3.34	3.65	3.42	5.08	12.94	0.13	13.11
CaO	1.18	5.66	15.94	0.18	0.34	13.68	9.17	0.10	0.18	48.10	0.16	17.86	9.64	1.99
Na_2O	0.06	0.09	0.23	0.04	–	3.57	5.06	0.09	0.06	1.37	0.01	0.30	3.44	0.07
K2O	0.05	0.01	–	0.03	–	0.04	0.18	0.02	–	0.02	–	0.01	0.14	0.22
Cr_2O_3	0.54	0.46	0.74	0.13	0.01	0.06	0.09	49.71	24.70	0.02	0.56	0.81	–	0.09
V_2O_3	0.03	0.04	0.03	–	–	0.02	0.03	0.56	0.72	0.10	0.74	0.09	–	0.03
NiO	0.07	0.01	–	0.02	–	–	0.09	0.09	–	0.03	–	–	–	0.09
P_2O_5	0.01	–	–	0.05	–	–	–	0.06	–	44.80	0.01	–	0.89	0.20
Total	100.49	100.08	99.39	99.61	100.52	100.61	100.37	100.62	100.67	99.64	100.40	100.55	99.71	88.64

1 = Ca-poor pyroxene core ($En_{78.7}Fs_{19.0}Wo_{2.3}$). 2 = Ca-poor pyroxene rim ($En_{57.9}Fs_{30.4}Wo_{11.7}$). 3 = Augite ($En_{47.2}Fs_{18.8}Wo_{33.9}$). 4 = Olivine core ($Fo_{75.2}$). 5 = Olivine rim ($Fo_{58.9}$). 6 = Plagioclase (An-rich) ($An_{67.8}Ab_{32.0}Or_{0.2}$). 7 = Plagioclase (An-poor) ($An_{49.5}Ab_{49.4}Or_{1.1}$). 8 = Spinel (Cr-rich). 9 = Spinel (Ti-rich). 10 = Merrillite (containing 0.61 wt% F). 11 = Ilmenite. 12 = Pyroxene in the magmatic inclusion within olivine. 13 = Feldspathic glass in the magmatic inclusion within olivine. 14 = Unknown (iddingsite?) (containing 0.06 wt% Cl and 0.01 wt% F).

show a slight increase from the core to the rim (Fig. 4). Nickel oxide (NiO) is also detected in olivine (0.06 wt%). Chromium is enriched in the core (Cr_2O_3: 0.3 wt%) compared with the rim (Cr_2O_3: 0.05 wt%). However, there are many chromite inclusions within olivine and this may cause Cr-rich analysis of some cores.

Pyroxene–Pyroxene compositions fall in the range of orthopyroxene, pigeonite and augite. However, it is unclear whether pyroxene falling in the typical orthopyroxene compositional range is orthorhombic or not. Low-Ca pyroxene shows a systematic chemical zoning trend from magnesian cores ($En_{76}Fs_{21}Wo_3$) to slightly calcic-ferroan rims ($En_{58}Fs_{30}Wo_{12}$), although zoning textures within the grain are rather irregular (Fig. 5). Minor elements are also zoned, but they are not so systematic as Fe and Mg. The compositional ranges are generally similar to those of Zipfel *et al.* (2000). Al_2O_3 mostly ranges from 0.3 to 1.5 wt%, but some are up to 2–2.5 wt%. TiO_2 is mostly around 0.1–0.8 wt%. Cr_2O_3 ranges from 0.7 to 0.5 wt%. Augite shows slight chemical zoning, but is clustered around the composition of $En_{50}Fs_{18}Wo_{32}$ (Fig. 5). X-ray elemental mapping by electron microprobe suggests that low-Ca pyroxenes (orthopyroxene and pigeonite) and high-Ca pyroxene (augite) are most commonly present as separate grains, rather than being in core-rim relationships within single grains (Fig. 6). However, this is not always clear because pyroxene shows irregular zoning patterns and is also shock metamorphosed (*e.g.*, Greshake and Stöffler, 1999). For example, in contrast to our observation, Zipfel *et al.* (1999) reported that augite occurs as both cores of pyroxene mantled by pigeonite and as overgrowth on pigeonite cores. Two-pyroxene thermometry employed for a pigeonite-augite pair gives an equilibration temperature of about 1100 °C (Lindsley and Andersen, 1983).

Plagioclase–Plagioclase glass shows a small compositional variation from one grain to another (An_{70-50}), but most grains are more An-rich than An_{60} (Fig. 5). Their zoning patterns as well as their textural forms are highly irregular, and some grains contain Na-rich regions in their rim areas (Fig. 6). Plagioclase contains 0.4–0.8 wt% FeO and 0.1–0.3 wt% MgO, respectively. Because of the irregular shape of plagioclase grains, spatial zoning patterns of these elements are unclear. However, Fe is usually enriched in the Na-rich regions.

Minor phases–Spinels are Cr-rich and are chemically zoned. They are divided into two types. One is Cr-rich and Ti-poor spinel and the other is Ti-rich spinel. Especially, Ti-rich spinel shows remarkable chemical zoning towards the rim of ulvöspinel-rich component. Although chromites occur within both olivine megacrysts and groundmass, there are no significant differences in composition. Merrillite is homogeneous and microprobe analysis gives the composition of $Ca_{8.85}(Mg,Fe)_{1.05}Na_{0.27}(PO_4)_7$ with minor amounts of F (0.6 wt%). Ilmenite contains about 5 wt% MgO. Magmatic inclusions within olivine are mainly composed of Al-Ti-rich pyroxene and Si-rich feldspathic glass. Pyroxene contains

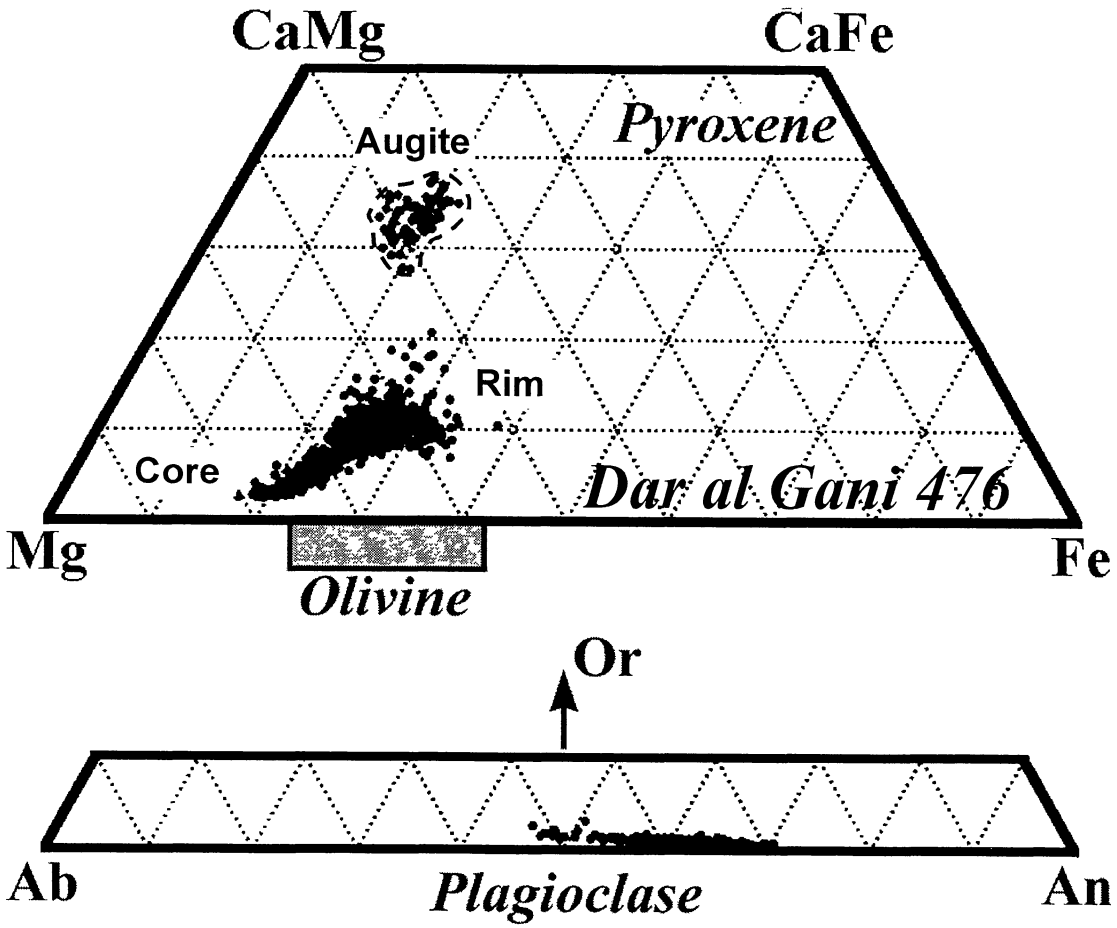

FIG. 5. Pyroxene quadrilateral and feldspar compositions of Dar al Gani 476. The range of olivine compositions is also shown as a box (atomic Fe/(Fe + Mg) ratio) at the bottom of the pyroxene quadrilateral.

~10 wt% Al_2O_3 and ~2 wt% TiO_2. Carbonates are nearly pure calcite composition and are $Cal_{97}Mag_2Sid_1$. An unknown Fe-rich phase (total: 88 wt%) is observed at the rims of a few large olivine grains. This phase is fairly heterogeneous in composition and irregularly shaped. Its composition is roughly similar to "iddingsite" in nakhlite olivines and may be a weathering product of olivine (*e.g.*, Boctor *et al.*, 1976). Greshake and Stöffler (1999) also reported the presence of iddingsite in Dar al Gani 476.

DISCUSSION

Mineralogical Comparison with Other Shergottitic Martian Meteorites

This study reveals that Dar al Gani 476 shows close affinities to lithology A of EETA79001 in the following respects (also pointed out by Mikouchi, 1999 and Zipfel *et al.*, 2000): (1) Overall basaltic texture. (2) The presence of olivine megacrysts reaching 5 mm across (Steele and Smith, 1982; McSween and Jarosewich, 1983). (3) Fine-grained groundmass mainly composed of pyroxene prisms with lesser amounts of anhedral plagioclase (interstitial to pyroxene). (4) Extensive shock effects causing formation of "maskelynitized" plagioclase and other typical shock metamorphic textures. (5) Mineral compositions of olivine, pyroxene, plagioclase, spinel, merrillite and ilmenite (Steele and Smith, 1982; McSween and Jarosewich, 1983). (6) Presence of magmatic inclusions in olivine, composed of Al-Ti-rich pyroxene and Si-rich feldspathic glass. It should be also noted that mineral compositions of olivine megacrysts, pyroxene, spinel and ilmenite generally agree with those found in the lherzolitic martian meteorites (ALH 77005, LEW 88516 and Y-793605) (*e.g.*, Harvey *et al.*, 1993; Treiman *et al.*, 1994; Mikouchi and Miyamoto, 1997).

Nevertheless, it is also clear that Dar al Gani 476 is somewhat distinct from lithology A of EETA79001. Low-Ca pyroxene in the Dar al Gani 476 groundmass ($En_{76}Fs_{21}Wo_3$~$En_{58}Fs_{30}Wo_{12}$) is more magnesian than that in lithology A of EETA79001 ($En_{73}Fs_{22}Wo_5$~$En_{45}Fs_{43}Wo_{12}$) (Fig. 7). Its composition is rather similar to that of pyroxene in lherzolitic martian meteorites

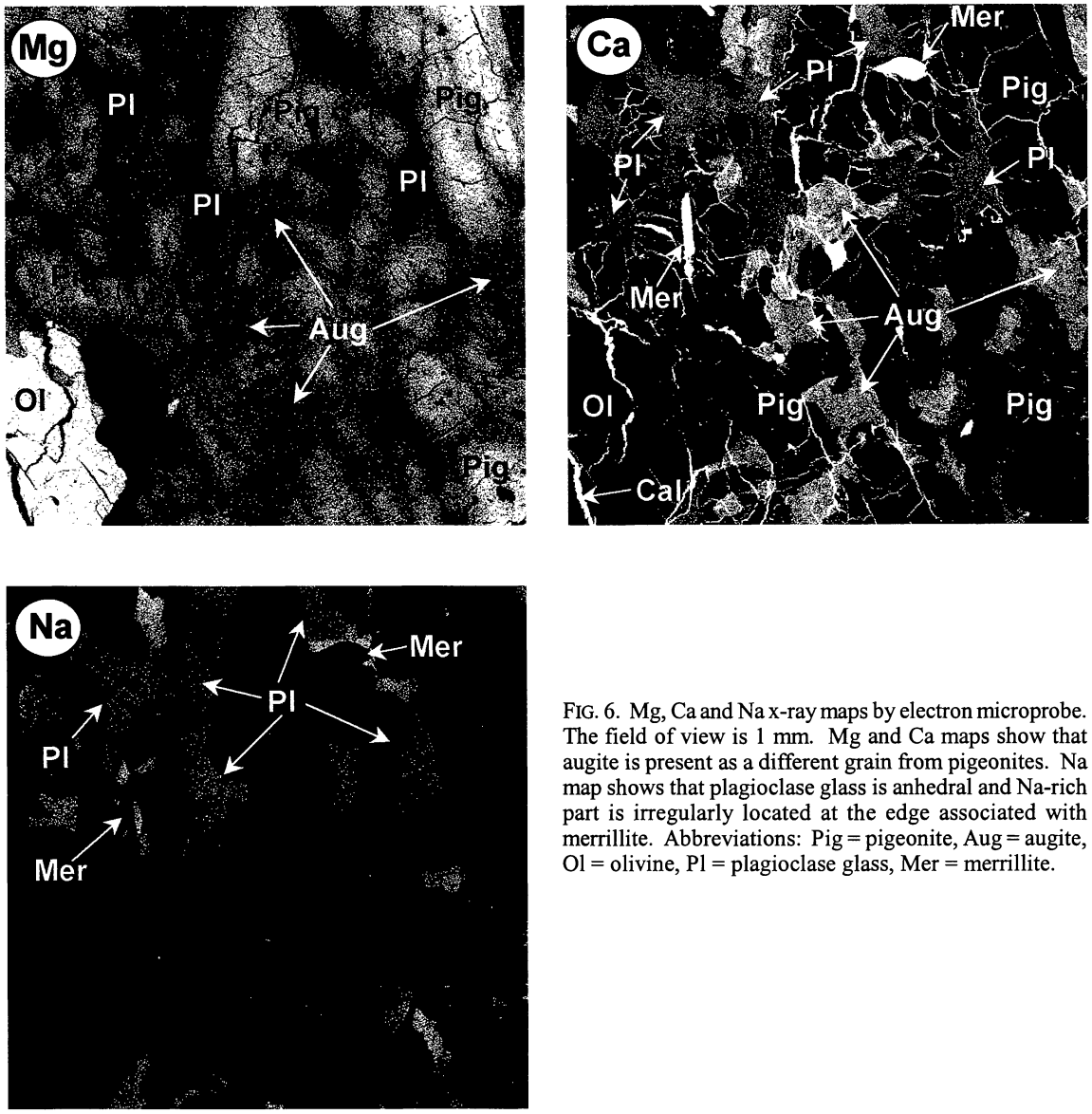

FIG. 6. Mg, Ca and Na x-ray maps by electron microprobe. The field of view is 1 mm. Mg and Ca maps show that augite is present as a different grain from pigeonites. Na map shows that plagioclase glass is anhedral and Na-rich part is irregularly located at the edge associated with merrillite. Abbreviations: Pig = pigeonite, Aug = augite, Ol = olivine, Pl = plagioclase glass, Mer = merrillite.

($En_{76}Fs_{21}Wo_3$~$En_{63}Fs_{22}Wo_{15}$) (*e.g.*, Harvey *et al.*, 1993; Treiman *et al.*, 1994; Mikouchi and Miyamoto, 1997) (Fig. 7). Furthermore, low-Ca pyroxene and augite in the Dar al Gani 476 groundmass are present as separate grains unlike lithology A of EETA79001 (Mikouchi *et al.*, 1999b). This may mean that Dar al Gani 476 experienced slightly less undercooling of the magma than did lithology A of EETA79001. Dar al Gani 476 olivine shows a narrower compositional range (Fo_{76-58}) than EETA79001 olivine (Fo_{81-53}) and is more similar to olivines in lherzolitic martian meteorites (Fo_{74-65}) (Fig. 8). However, olivines in lherzolitic martian meteorites are typically unzoned, and compositions of olivine and pyroxenes extend to more Fe-rich compositions in Dar al Gani 476 than those phases in lherzolitic martian meteorites. Plagioclase glass in Dar al Gani 476 is more An-rich than that in lithology A of EETA79001 and is the most An-rich of all the shergottitic martian meteorites. Late-crystallized phases (*e.g.*, merrillite) are also less abundant compared with lithology A of EETA79001. Furthermore, as noted by Zipfel *et al.* (2000), the orthopyroxene-olivine-chromite xenolith typically found in the lithology A of EETA79001 is absent in Dar al Gani 476. It appears that Dar al Gani 476 crystallized from a more primitive mafic magma than lithology A of EETA79001. At least several phases (olivine, pyroxene, chromite, and ilmenite) in Dar al Gani 476 suggest petrogenetic similarities to lherzolitic martian meteorites.

FIG. 7. Minor element distributions in Dar al Gani 476 pyroxenes. (a) Wt% Al_2O_3 *vs.* atomic Fe/(Fe + Mg). (b) Wt% TiO_2 *vs.* atomic Fe/(Fe + Mg). For comparison, pyroxenes from lithology A of EETA79001 and Y-793605 martian lherzolite are also plotted. The diagrams show that Dar al Gani 476 pyroxenes have intermediate compositions between EETA79001 and Y-793605 pyroxenes.

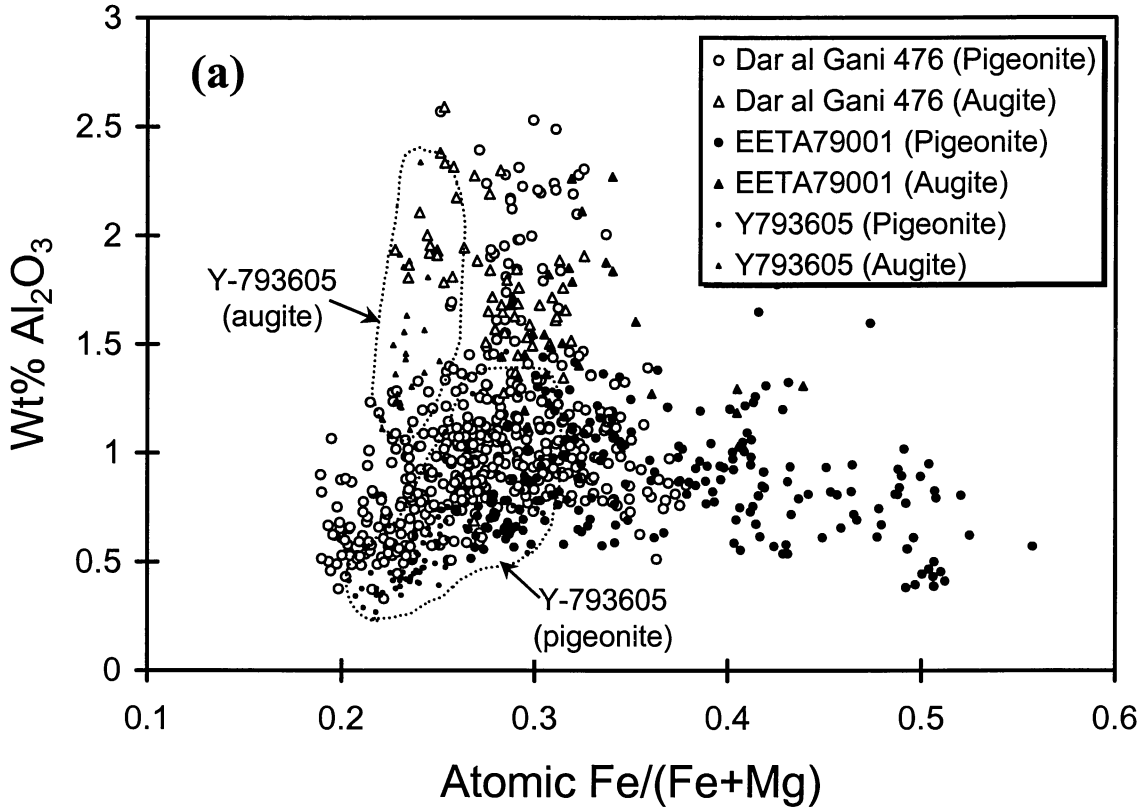

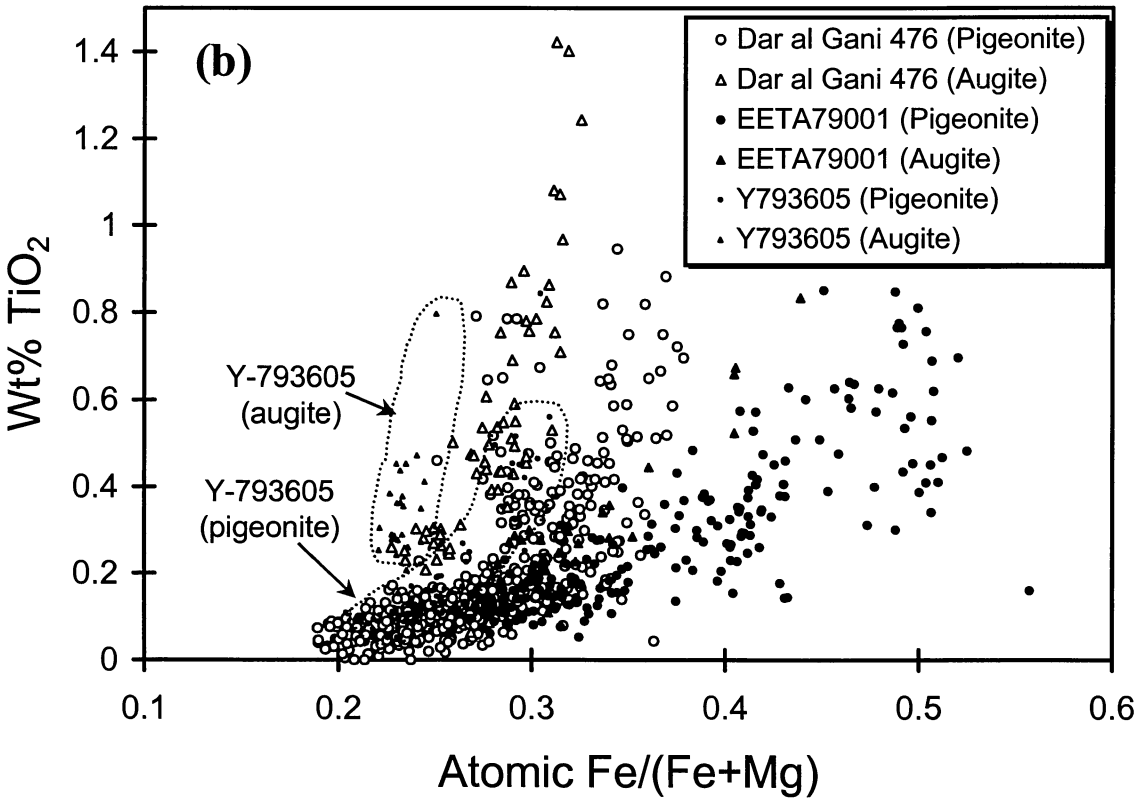

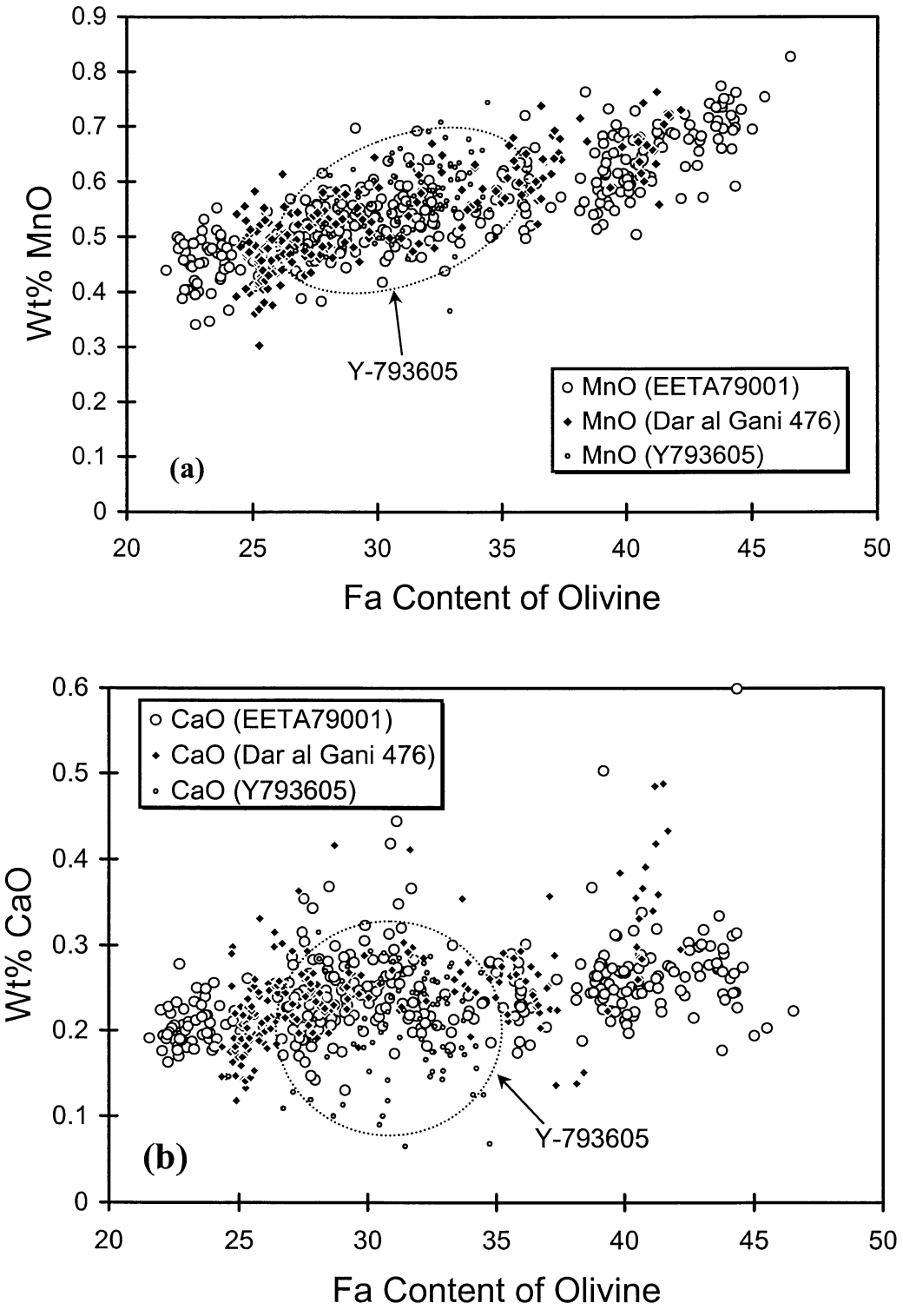

FIG. 8. Minor element distributions in Dar al Gani 476 olivines. (a) Wt% MnO *vs.* Fa content. (b) Wt% CaO *vs.* Fa content. (c) Wt% Cr_2O_3 *vs.* Fa content. (d) Wt% NiO *vs.* Fa content. For comparison, olivines from lithology A of EETA79001 and Y-793605 martian lherzolite are also plotted. All olivines show overlap in minor elements at similar Fe/Mg. Y-793605 olivine shows very restricted range in Fe/Mg, while olivines in Dar al Gani 476 and lithology A of EETA79001 show much larger range.

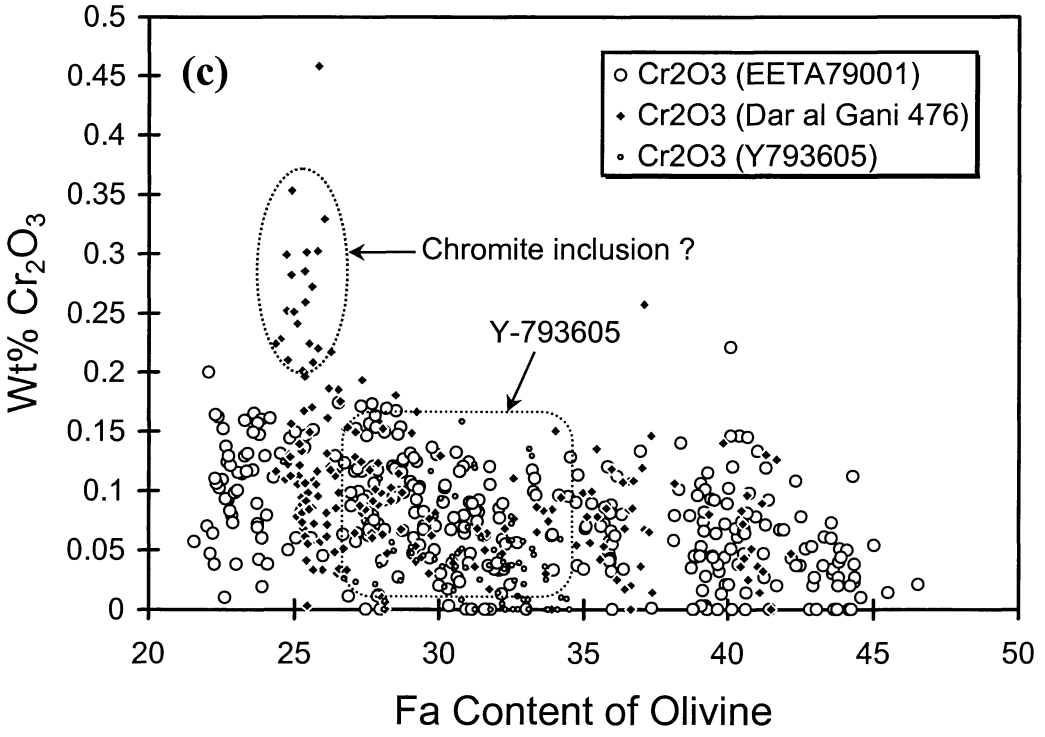

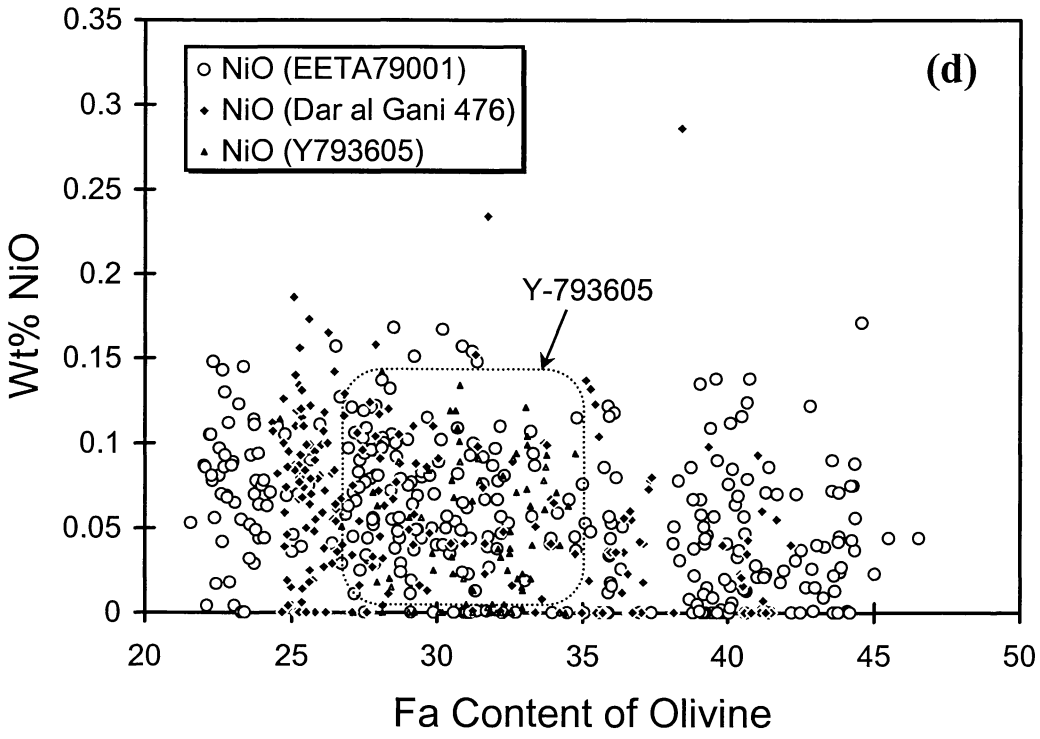

FIG. 8. *Continued.*

Recently, Mittlefehldt *et al.* (1999) proposed that lithology A of EETA79001 is an impact melt that is a simple mixture of ~44% EETA79001 lithology B and ~56% of ALH 77005 (or Y-793605) light lithology. It is not clear from this study whether Dar al Gani 476 is also an impact melt or not, but this idea appears consistent with the fast cooling discussed in the following section. Unfortunately, the petrology and mineralogy of Dar al Gani 476 do not support the apparent relationship to QUE 94201, nakhlites and Chassigny that is suggested by the isotopic and trace element data (Jagoutz *et al.*, 1999; Zipfel *et al.*, 1999; Wadhwa *et al.*, 1999). Instead, they indicate a relationship to lithology A of EETA79001 and lherzolitic martian meteorites. It is especially remarkable that differences between Dar al Gani 476 and lithology A of EETA79001 are smaller than those between two lithologies (A and B) in EETA79001. Thus, it is almost as if Dar al Gani 476 had a geological contact with lithology A of EETA79001 and these two rocks came from the same igneous body on Mars. However, other data rule this scenario out: the crystallization age of Dar al Gani 476 is about 750–800 Ma and is distinct from that of EETA79001 (Jagoutz *et al.*, 1999; Wooden *et al.*, 1982). Also, the cosmic exposure age of Dar al Gani 476 is about 1.2 Ma, which is significantly older than that of EETA79001 (about 0.65 Ma), suggesting that they represent different ejection events (Scherer and Schultz, 1999).

Olivine in Dar al Gani 476, Phenocrysts or Xenocrysts?

Although olivine megacrysts in Dar al Gani 476 are chemically zoned from Fo_{76} cores to Fo_{62} rims, smaller anhedral olivine is chemically homogenous (Fo_{62-58}). There is no distinct difference in volumetric abundance between large euhedral grains and small anhedral grains. Intermediate-sized grains showing slight zoning are also present. Some of these intermediate grains have their most magnesian parts at their edges (Fig. 9). Zipfel *et al.* (2000) suggested that olivines in Dar al Gani 476 can be grouped into three: $Fo_{\sim 74}$, Fo_{70-68}, and Fo_{68-64}. However, it was not clear in the section studied here. Olivine megacrysts in the lithology A of EETA79001 have wider compositional ranges (Fo_{81-55}) than those in Dar al Gani 476 (Fig. 8) although both show generally similar petrographic and mineralogical characteristics. Olivine megacrysts in lithology A of EETA79001 are interpreted to be xenocrysts (Steele and Smith, 1982; McSween and Jarosewich, 1983). Minor elements in EETA79001 olivine are similar in abundance to those in Dar al Gani 476, as shown in Fig. 8.

Assuming that $kD^{\text{Atomic Fe/Mg}}_{\text{olivine/melt}}$ is 0.35 (Stolper, 1977), a melt having the bulk composition of Dar al Gani 476 (atomic Mg/(Mg + Fe) = 0.68 from Zipfel *et al.* (2000)) would be in equilibrium with olivine of Fo_{86}. This is more magnesian than the observed olivine core composition (Fo_{76}). We also

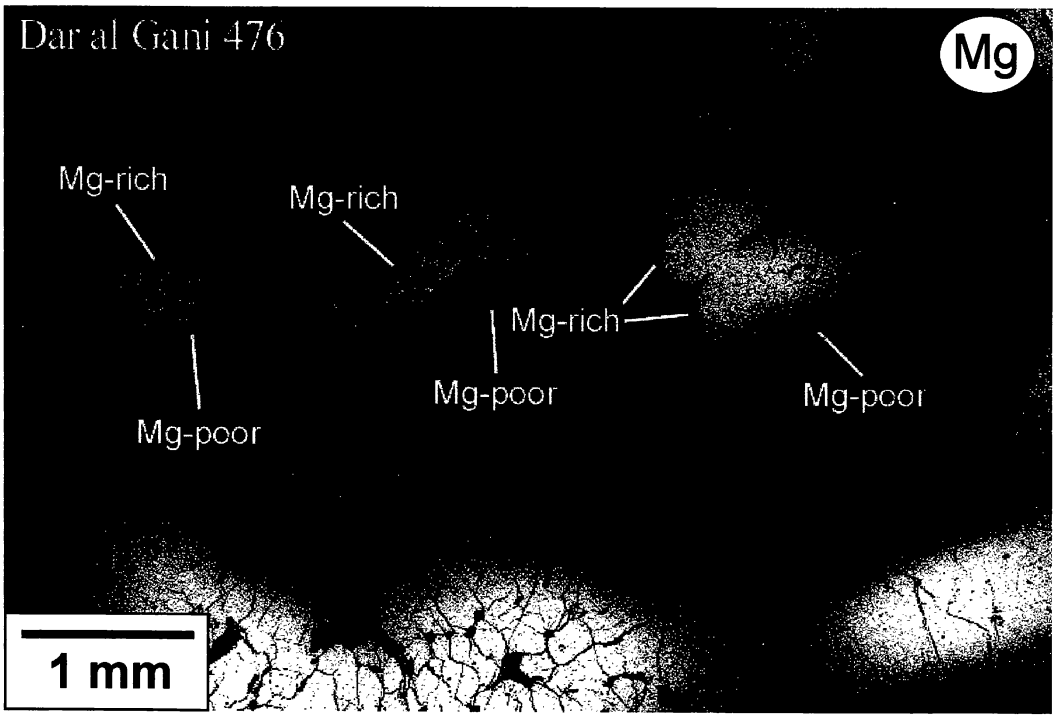

FIG. 9. Mg x-ray map of Dar al Gani 476. Bright areas are olivines. Note that some olivines have the most magnesian parts at their edges, as though a grain with normal core-to-rim zoning was fractured, exposing the core to groundmass.

calculated the olivine composition in equilibrium with the groundmass having atomic Mg/(Mg + Fe) of 0.61 (average composition of several microprobe line analyses of the groundmass). The resultant composition is Fo_{82}. In either case, these calculated compositions are more magnesian than the most magnesian core composition of Dar al Gani 476 olivine. Therefore, from this calculation, we cannot distinguish between origin as phenocrysts or xenocrysts. It is possible to say that olivine grains in Dar al Gani 476 are either xenocrysts or they can be phenocrysts that crystallized after the crystallization of more magnesian phases (probably orthopyroxene). Zipfel *et al.* (2000) pointed out that the olivine core is not Mg-rich enough to be in equilibrium with orthopyroxene. Thus, the bulk composition of Dar al Gani 476 may represent a melt composition and olivine may be phenocrysts crystallizing from the melt after orthopyroxene. In order to test this, we also calculated the pyroxene composition which is in equilibrium with the bulk atomic Mg/(Mg + Fe) composition of 0.68 by using $kD^{\text{Atomic Fe/Mg}}_{\text{pyroxene/melt}}$ of 0.30 (Stolper, 1977). The resulting equilibrated atomic Mg/(Mg + Fe) composition of pyroxene is 0.88. Because the most magnesian orthopyroxene core has an atomic Mg/(Mg + Fe) composition of 0.80, the calculated composition is also more magnesian than the observed one. One possible explanation for this discrepancy would be if the core compositions of the phenocrysts were continuously modified to more Fe-rich compositions by diffusion as the melt evolved during cooling and crystallization. However, the presence of Mg-rich olivine cores adjacent to groundmass in olivine fragments suggests that cooling was too rapid to allow significant diffusive modification of olivine cores. Because diffusion in pyroxene is orders of magnitude slower than in olivine (Jurewicz and Watson, 1988; Fujino *et al.*, 1990), this observation even more strongly precludes significant modification of pyroxene cores. Nevertheless, it is probable that olivine might grow as "phenocryst" at different time and place from the groundmass. In that case, perfect equilibrium is seldom achieved. For example, all sorts of complexities may occur within the context of a (potentially zoned) magma chamber and its associated plumbing that would lead to an appreciable disequilibrium between early crystals of magma chamber and the groundmass of one of its daughter lavas. Thus, it is difficult to conclude the origin of olivine megacrysts in Dar al Gani 476 either phenocryst or xenocryst.

Cooling Rates of Dar al Gani 476 and Elephant Moraine A79001 Olivines

The presence of fragment-like olivine grains having Mg-rich composition at the edge shows evidence that the zoning pattern is of mostly primary igneous origin (Fig. 9). By assuming that olivine crystallized by a closed-system fractional crystallization process and then was slightly modified by atomic diffusion due to contact with the surrounding melt, we estimated cooling rates of Dar al Gani 476 and EETA79001 olivines by employing a method similar to that of Miyamoto *et al.* (1986). We can also find olivine megacrysts in EETA79001 that have a Mg-rich composition at their edges. Because olivine megacrysts in Dar al Gani 476 and EETA79001 have smooth systematic chemical zoning, we assumed a fractional crystallization model that allows easy calculation of the zoning profile (Jones, 1990; Kaiden *et al.*, 1998). Although we assumed that initial zoning profile was formed by a fractional crystallization, this assumption is not critical to our estimate of cooling rates. Even if the original zoning was steeper, the resultant cooling rates will differ only by one order of magnitude at most.

Although several data have been reported for a Mg-Fe diffusion rate in olivine (*e.g.*, Buening and Buseck, 1973; Misener, 1974; Chakraborty, 1997), we used one by Misener (1974) because our recent diffusion experiments (Miyamoto and Mikouchi, 1998) give the best fit between observed diffusion profiles and those using the diffusion rate $D_{\text{Mg-Fe in olivine}}$ from Misener (1974). We revised the equation of Misener (1974) by dependence of oxygen fugacity (we employed fO_2 at the QFM buffer because it is the estimated fO_2 of Shergotty and Zagami (Stolper and McSween, 1979)) and Fe/Mg ratios upon the diffusion rates (Miyamoto and Mikouchi, 1998). Although the recent diffusion experiments of Chakraborty (1997) gave a slower Mg-Fe diffusion rate of up to two orders of magnitude, the revised diffusion rate reduce the discrepancy down to $10^{0.8}$ at 1300 °C and $10^{1.1}$ at 1200 °C between Misener (1974) and Chakraborty (1997) if we consider difference of fO_2 (fO_2 = 10^{-12} in Chakraborty (1997) *vs.* log fO_2 = QFM in this calculation). We calculated diffusion profiles for cooling over the temperature ranges of 1300–700 °C and 1200–700 °C. Even if olivine cooled down to lower than 700 °C, there is no significant difference in the result because atomic diffusion rate at such a low temperature is much slower and profile modification is mostly achieved at high temperature (>1100 °C). Olivine may have started cooling from a higher temperature than 1300 °C. In that case, olivine should have experienced faster cooling rates than the cooling rates from either 1300 or 1200 °C.

Dar al Gani 476–The profile produced by fractional crystallization broadly agrees with the observed profile when the remaining liquid amount is 40 vol%. However, a slight disturbance near the edge may suggest diffusive modification due to the contact with the magma. The calculated profiles (by Mg-Fe diffusion rate by Misener, 1974) are shown in Fig. 10 with the observed profile and the results are summarized in Table 2. The cooling rate of 15 °C/h (1300–700 °C) nearly preserves the chemical zoning of olivine megacrysts produced by fractional crystallization. The cooling rate of 3 °C/h (1300–700 °C) gives the best fit to the observed profile. Cooling rates slower than 1.5 °C/h (1300–700 °C) significantly modify the primary profile and do not agree with the observed profile. For the temperature range of 1200–700 °C, the cooling rate of 4 °C/h nearly preserves the original zoning produced by fractional

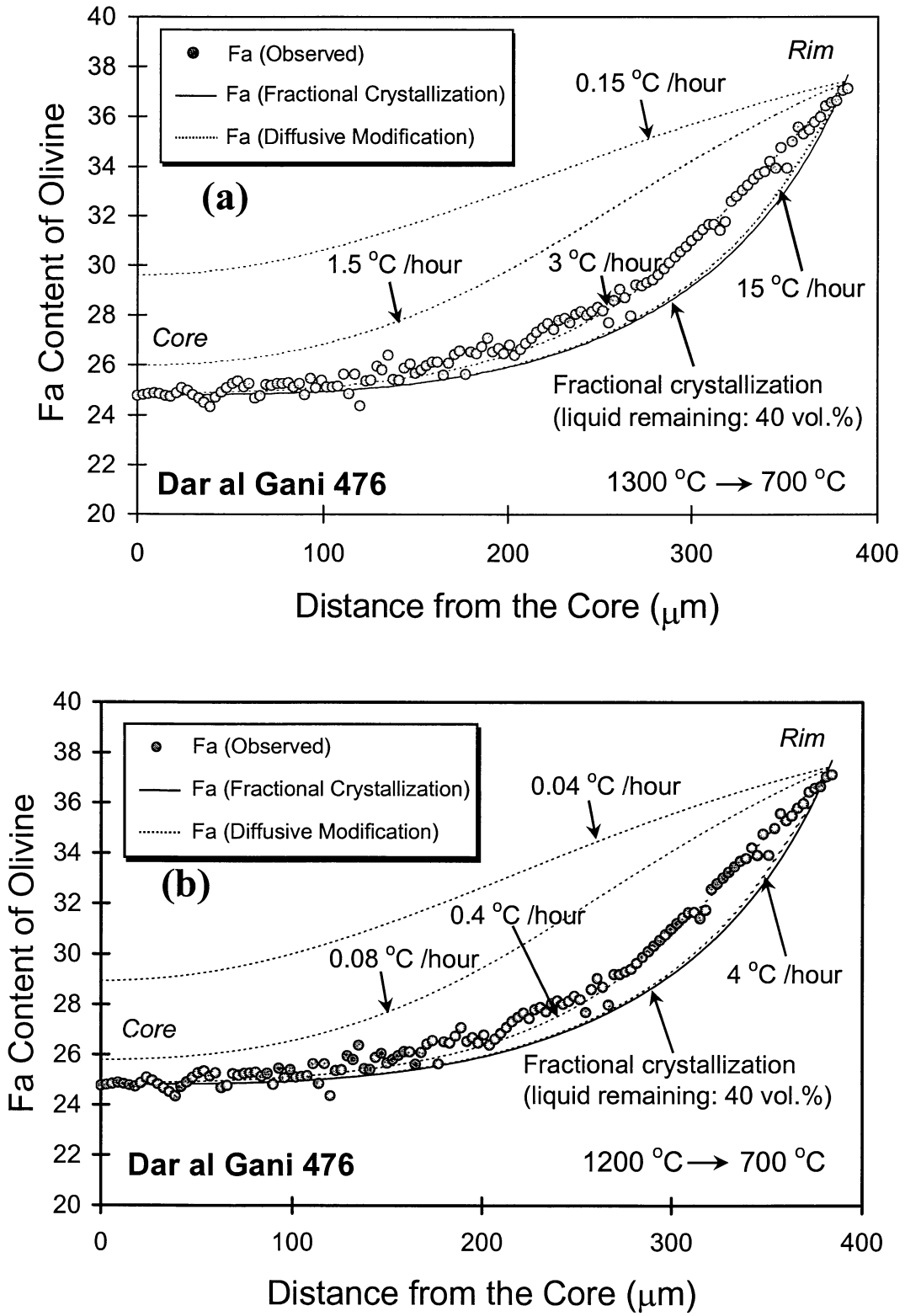

FIG. 10. The results from the cooling rate calculation for Dar al Gani 476 olivine by using diffusion rates by Misener (1974). (a) Cooling from 1300 to 700 °C. The solid line is a calculated profile assuming a fractional crystallization and the dashed lines are diffusionally modified profiles from the initial profile (same for Figs. 10b and 11a,b). The cooling rate of 3 °C/h gives the best fit. (b) Cooling from 1200 to 700 °C. The cooling rate of 0.4 °C/h gives the best fit.

TABLE 2. Best-fit olivine cooling rates for Dar al Gani 476 and EETA79001.

	Temperature range	Mg-Fe diffusion data	Best-fit cooling rate	Burial depth
Dar al Gani 476				
	1300–700 °C	Misener (1974)	3 °C/h	0.8 m
	1300–700 °C	Chakraborty (1997)	0.5 °C/h	1.2 m
	1200–700 °C	Misener (1974)	0.4 °C/h	1.3 m
	1200–700 °C	Chakraborty (1997)	0.03 °C/h	3 m
EETA79001				
	1300–700 °C	Misener (1974)	5 °C/h	0.7 m
	1300–700 °C	Chakraborty (1997)	0.8 °C/h	1 m
	1200–700 °C	Misener (1974)	0.4 °C/h	1.3 m
	1200–700 °C	Chakraborty (1997)	0.05 °C/h	2.5 m

crystallization. The cooling rate of 0.4 °C/h (1200–700 °C) gives the best-fit profile to the observed Dar al Gani 476 olivine. Cooling rates slower than 0.08 °C/h produce major changes in the original profile and do not fit the observed profile. Therefore, these results indicate that the Dar al Gani 476 olivine cooled faster than these cooling rates. The cooling rates of 3 °C/h (1300–700 °C) and 0.4 °C/h (1200–700 °C) correspond to the burial depths of 0.8 and 1.3 m, respectively if we assumed that they were covered with rock-like materials. If they were covered with regolith-like materials, burial depths are much shallower due to lower thermal diffusivity (*e.g.*, McKay *et al.*, 1998). If we employed diffusion rates by Chakraborty (1997), the obtained best-fit cooling rates are 0.5 °C/h (1300–700 °C) and 0.03 °C/h (1200–700 °C). These cooling rates correspond to the burial depths of about 1.2 and 3 m, respectively. Thus, it is likely that Dar al Gani 476 cooled in a lava flow to satisfy a geological setting giving such small burial depths from the martian surface. Probably, the partial foliation texture of olivine and pyroxene resulted from flow alignment in the lava. Recently, Lentz and McSween (2000) estimated a crystallization process of Dar al Gani 476 and EETA79001 (lithology A) groundmass by crystal size distribution analysis of pyroxene. They inferred fairly rapid crystallization during single stages of continuous nucleation and growth. Their results match with our calculation presented here.

Elephant Moraine A79001–The calculated profile produced by fractional crystallization generally agrees with the observed profile with the remaining liquid amount of 26 vol%. We computed a profile that was modified by atomic diffusion as we did for Dar al Gani 476 olivine. The calculated profiles (by using Mg-Fe diffusion rate by Misener, 1974) are shown in Fig. 11. The results are summarized in Table 2 along with Dar al Gani 476. The cooling rate that preserves the chemical zoning by fractional crystallization is about 20 °C/h for the temperature range from 1300 to 700 °C. The cooling rate of 5 °C/h gives the best fit to the observed profile of EETA79001 olivine. The cooling rates slower than 2 °C/h clearly modify the profile to more ferroan composition than the observed one. The cooling rate that prevents modification of fractional crystallization zoning is about 4 °C/h. The best-fit cooling rate is 0.4 °C/h and slower than the 0.08 °C/h cooling that nearly homogenizes the profile. Therefore, these results indicate that the EETA79001 olivine cooled faster than 0.4–5 °C/h. The cooling rates of 5 °C/h (1300–700 °C) and 0.4 °C/h (1200–700 °C) correspond to the burial depths of 0.7 and 1.3 m, respectively, if we assumed that they were covered with rock-like materials. The cooling rates of 0.4–5 °C/h for the olivine xenocrysts in EETA79001 are slightly faster than the previous report by Kaiden *et al.* (1998) (0.07–0.6 °C/h). This is because Kaiden *et al.* (1998) assumed that original profile was homogeneous and the zoning profile was produced by diffusional modification. We believe that the calculation in this study is more valid to estimate cooling history of EETA79001 than Kaiden *et al.* (1998) because of the presence of fragmental olivine grains having Mg-rich compositions in contact with EETA79001 groundmass. At any rate, the obtained cooling rates of 0.4–5 °C/h nearly agree with the results for Dar al Gani 476 olivine (Table 2). If we employed diffusion rates by Chakraborty (1997), the obtained best-fit cooling rates are 0.8 °C/h (1300–700 °C) and 0.05 °C/h (1200–700 °C). These cooling rates correspond to the burial depths of about 1 and 2.5 m, respectively. Hence, we suggest that Dar al Gani 476 and lithology A of EETA79001 experienced similar rapid cooling histories during the crystallization of their groundmass.

CONCLUSIONS

Dar al Gani 476 is similar to lithology A of EETA79001 in petrology and mineralogy, yet shows obvious differences from lithology A of EETA79001. Olivine megacrysts in Dar al Gani 476 are important in considering a possible relationship to lithology A of EETA79001. It is difficult to conclusively determine whether olivines in Dar al Gani 476 are phenocrysts or xenocrysts, even if their compositions are out of equilibrium with the bulk melt composition and they have a texture indicating partial intrusion of the groundmass melt into the olivine grains.

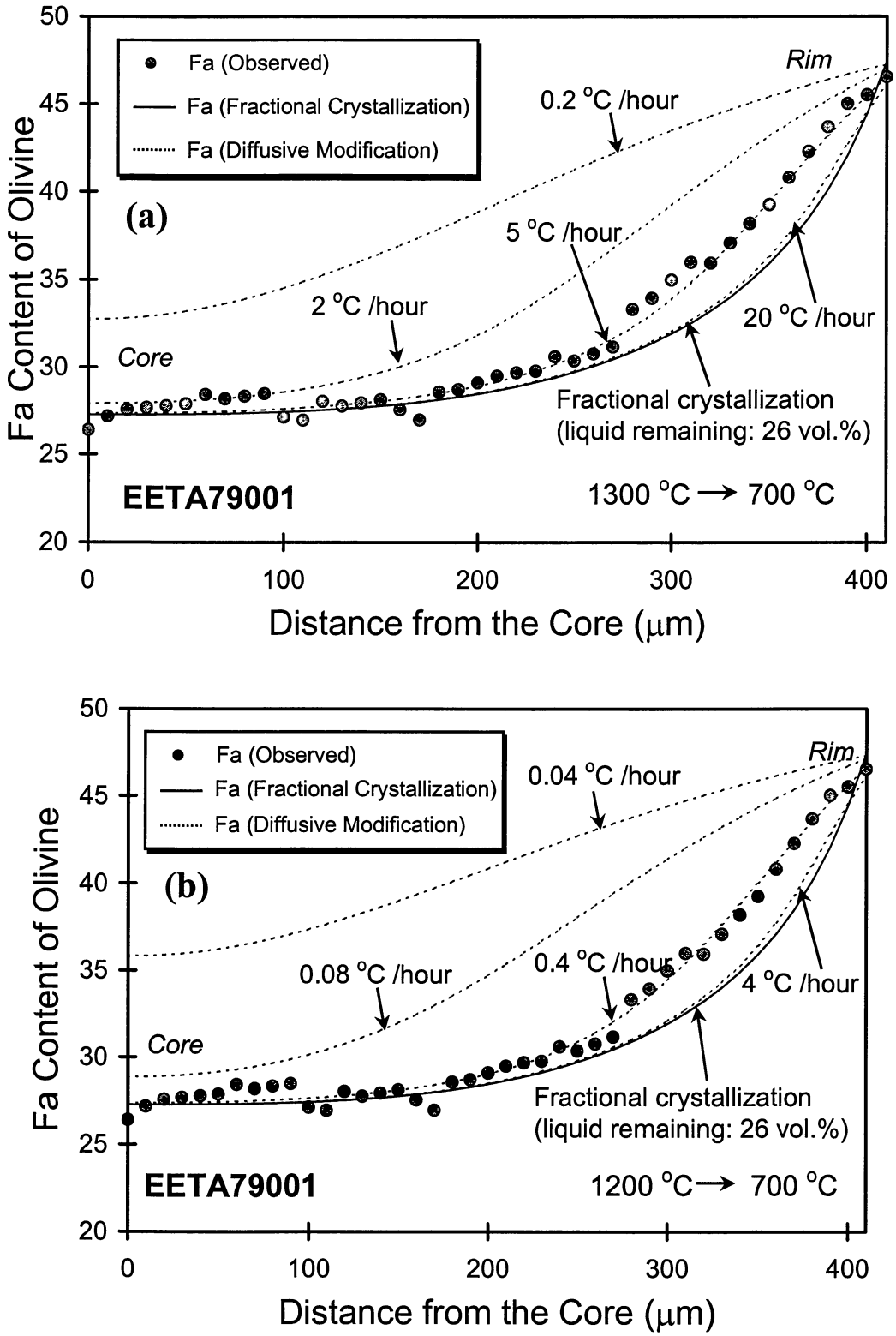

FIG. 11. The results from the cooling rate calculation for EETA79001 olivine by using diffusion rates by Misener (1974). (a) Cooling from 1300 to 700 °C. The cooling rate of 5 °C/h gives the best fit. (b) Cooling from 1200 to 700 °C. The cooling rate of 0.4 °C/h gives the best fit.

The cooling rate calculations suggest that olivines in both Dar al Gani 476 and EETA79001 cooled faster than 0.03 °C/h, indicating that they were cooled near the martian surface (shallower than about 3 m in depth at most). We consider it likely that they were cooled in lava flows and shared very similar groundmass crystallization histories. As Mittlefehldt *et al.* (1999) pointed out, impact melting is one plausible explanation for such a geological setting. The trace element study by Wadhwa *et al.* (1999) suggests that Dar al Gani 476 olivine is similar to EETA79001. Thus, there maybe a petrogenetic relationship between Dar al Gani 476 olivines and olivines in lherzolitic martian meteorites. On the other hand, trace element chemistry of the Dar al Gani 476 groundmass shows a similarity to QUE 94201 (Wadhwa *et al.*, 1999). The Mittlefehldt (1999) model assumes that lithology A of EETA79001 is a mixture of EETA79001 lithology B and ALH 77005 light lithology. By analogy, Dar al Gani 476 may be a mixture of martian lherzolite and other martian rock (*e.g.*, QUE 94201, nakhlites?). Nevertheless, Dar al Gani 476 and lithology A of EETA79001 had very similar cooling histories during groundmass crystallization. Further study, especially isotope and trace element chemistry, is required to clarify the petrogenetic relationship between Dar al Gani 476 and other martian meteorites.

Acknowledgements–We thank Prof. T. Tagai (The University Museum, University of Tokyo), Dr. J. Zipfel (Max-Planck-Institut für Chemie), the Meteorite Working Group (NASA Johnson Space Center) and National Institute of Polar Research (Tokyo, Japan) for supplying the meteorite samples. We also thank Drs. J. Zipfel, R. C. F. Lentz, and P. H. Warren for comprehensive and constructive reviews that improved the quality of the manuscript. The electron microscopy was performed in the Electron Microbeam Analysis Facility for mineralogy at Department of Earth and Planetary Science, University of Tokyo. This work was partially supported by the National Academy of Sciences through an NRC associateship at NASA Johnson Space Center and the Grant-in-Aid for Encouragement of Young Scientists by the Japanese Ministry of Education, Science and Culture (no. 12740297) (both to T. Mikouchi).

Editorial handling: P. H. Warren

REFERENCES

BECKER R. H. AND PEPIN R. O. (1984) The case for a martian origin of the shergottites: Nitrogen and noble gases in EETA79001. *Earth Planet. Sci. Lett.* **69**, 225–242.

BOCTOR N. Z., MEYER H. O. A. AND KULLERUD G. (1976) Lafayette meteorite: Petrology and opaque mineralogy. *Earth Planet. Sci. Lett.* **32**, 69–76.

BOGARD D. D. AND GARRISON D. H. (1998) Relative abundances of Ar, Kr and Xe in the martian atmosphere as measured in martian meteorites. *Geochim. Cosmochim. Acta* **62**, 1829–1835.

BOGARD D. D. AND JOHNSON P. (1983) Martian gases in an Antarctic meteorite. *Science* **221**, 651–654.

BUENING D. K. AND BUSECK P. R. (1973) Fe-Mg lattice diffusion in olivine. *J. Geophys. Res.* **78**, 6852–6862.

CHAKRABORTY S. (1997) Rate and mechanism of Fe-Mg interdiffusion in olivine at 980–1300 °C. *J. Geophys. Res.* **102**, 12 317–12 331.

CHEN M. AND EL GORESY A. (2000) The nature of maskelynite in shocked meteorites: Not diaplectic glass but a glass quenched from shock-induced dense melt at high pressures. *Earth Planet. Sci. Lett.* **179**, 489–502.

FOLCO L. AND FRANCHI I. A. (2000) Dar al Gani 670 shergottite: A new fragment of the Dar al Gani 476/489 martian meteorite (abstract). *Meteorit. Planet. Sci.* **35 (Suppl.)**, A54–A55.

FOLCO L., FRANCHI I. A., SCHERER P., SCHULTZ L. AND PILLINGER C. T. (1999) Dar al Gani 489 basaltic shergottite: A new find from the Sahara likely paired with Dar al Gani 476 (abstract). *Meteorit. Planet. Sci.* **34 (Suppl.)**, A36–A37.

FOLCO L., FRANCHI I. A., D'ORAZIO M., ROSSI S. AND SCHULTZ L. (2000) A new martian meteorite from the Sahara: The shergottite Dar al Gani 489. *Meteorit. Planet. Sci.* **35**, 827–839.

FUJINO K., NAOHARA H. AND MOMOI H. (1990) Direct determination of cation diffusion coefficients in pyroxene. *EOS* **71**, 943.

GRESHAKE A. AND STÖFFLER D. (1999) Shock metamorphic features in the SNC meteorite Dar al Gani 476 (abstract). *Lunar Planet. Sci.* **30**, #1377, Lunar and Planetary Institute, Houston, Texas, USA (CD-ROM).

GROSSMAN J. N. (1999) The Meteoritical Bulletin, No. 83, 1999 July. *Meteorit. Planet. Sci.* **34 (Suppl.)**, A169–A186.

GROSSMAN J. N. (2000) The Meteoritical Bulletin, No. 84, 2000 August. *Meteorit. Planet. Sci.* **35 (Suppl.)**, A199–A225.

HARVEY R. P., WADHWA M., MCSWEEN H. Y., JR. AND CROZAZ G. (1993) Petrography, mineral chemistry and petrogenesis of Antarctic shergottite LEW 88516. *Geochim. Cosmochim. Acta* **57**, 4769–4783.

JAGOUTZ E., BOGDANOVSKI O., KRESTINA N. AND JOTTER R. (1999) DaG: A new age in the SNC family, or the first gathering of relatives (abstract). *Lunar Planet. Sci.* **30**, #1808, Lunar and Planetary Institute, Houston, Texas, USA (CD-ROM).

JONES J. H. (1986) A discussion of isotopic systematics and mineral zoning in the shergottites: Evidence for a 180 m.y. igneous crystallization age. *Geochim. Cosmochim. Acta* **50**, 969–977.

JONES R. H. (1990) Petrology and mineralogy of Type II, FeO-rich chondrules in Semarkona (LL3.0): Origin by closed-system fractional crystallization, with evidence for supercooling. *Geochim. Cosmochim. Acta* **54**, 1785–1802.

JUREWICZ A. J. G. AND WATSON E. B. (1988) Cations in olivine, part 2: Diffusion in olivine xenocrysts, with application to petrology and mineral physics. *Contrib. Mineral. Petrol.* **99**, 186–201.

KAIDEN H., MIKOUCHI T. AND MIYAMOTO M. (1998) Cooling rates of olivine xenocrysts in the EET79001 shergottite. *Antarct. Meteorite Res.* **11**, 92–102.

LENTZ R. C. F. AND MCSWEEN H. Y., JR. (2000) Crystallization of the basaltic shergottites: Insights from crystal distribution (CSD) analysis of pyroxenes. *Meteorit. Planet. Sci.* **35**, 919–927.

LINDSLEY D. H. AND ANDERSEN D. J. (1983) A two-pyroxene thermometer. *Proc. Lunar Planet. Sci. Conf.* **13th**, *J. Geophys. Res.* **88 (Suppl.)**, A887–A906.

MCKAY G. A., MIYAMOTO M., MIKOUCHI T. AND OGAWA T. (1998) The cooling history of the LEW 86010 angrite as inferred from kirschsteinite lamellae in olivine. *Meteorit. Planet. Sci.* **33**, 977–983.

MCSWEEN H. Y., JR. (1994) What we have learned about Mars from SNC meteorites. *Meteoritics* **29**, 757–779.

MCSWEEN H. Y., JR. AND JAROSEWICH E. (1983) Petrogenesis of the Elephant Moraine A 79001 meteorite: Multiple magma pulses on the shergottite parent body. *Geochim. Cosmochim. Acta* **47**, 1501–1513.

MEYER C. (1998) *Mars Meteorite Compendium–1998.* NASA Johnson Space Center, Houston, Texas, USA. 237 pp.

MIKOUCHI T. (1999) Preliminary examination of Dar al Gani 476: A new basaltic martian meteorite similar to lithology A of

EETA79001 (abstract). *Lunar Planet. Sci.* **30**, #1557, Lunar and Planetary Institute, Houston, Texas, USA (CD-ROM).

MIKOUCHI T. AND MIYAMOTO M. (1997) Yamato-793605: A new lherzolitic shergottite from Japanese Antarctic meteorite collection. *Antarct. Meteorite Res.* **10**, 41–60.

MIKOUCHI T., MIYAMOTO M. AND MCKAY G. (1999a) Cooling rates of olivine in the martian meteorites Dar al Gani 476 and Elephant Moraine A79001 (abstract). *Meteorit. Planet. Sci.* **34 (Suppl.)**, A81–A82.

MIKOUCHI T., MIYAMOTO M. AND MCKAY G. (1999b) The role of undercooling in producing igneous zoning trends in pyroxenes and maskelynites among basaltic martian meteorites. *Earth Planet. Sci. Lett.* **173**, 235–256.

MISENER D. J. (1974) Cation diffusion in olivine to 1400 °C and 35 kbar. In *Geochemical Transport and Kinetics* (eds. A. W. Hoffmann, B. J. Giletti, H. S. Yoder, Jr. and R. A. Yund), pp. 117–129. Carnegie Inst. of Washington, Washington, D.C., USA.

MITTLEFEHLDT D. W., LINDSTROM D. J., LINDSTROM M. M. AND MARTINEZ R. R. (1999) An impact-melt origin for lithology A of martian meteorite Elephant Moraine A79001. *Meteorit. Planet. Sci.* **34**, 357–368.

MIYAMOTO M. AND MIKOUCHI T. (1998) Evaluation of diffusion coefficients of Fe-Mg and Ca in olivine. *Mineral. J.* **20**, 9–18.

MIYAMOTO M., MCKAY D. S., MCKAY G. A. AND DUKE M. B. (1986) Chemical zoning and homogenization of olivines in ordinary chondrites and implications for thermal histories of chondrules. *J. Geophys. Res.* **91**, 12 804–12 816.

NISHIIZUMI K., MASARIK J., WELTEN K. C., CAFFEE M. W., JULL A. J. T. AND KLANDRUD S. (1999) Exposure history of new Martian meteorite Dar al Gani 476 (abstract). *Lunar Planet. Sci.* **30**, #1966, Lunar and Planetary Institute, Houston, Texas, USA (CD-ROM).

OTT U. AND BEGEMANN F. (1985) Are all the "martian" meteorites from Mars? *Nature* **317**, 509–512.

REID A. M. AND SCORE R. (1981) A preliminary report on the achondrite meteorites in the 1979 U. S. Antarctic Meteorite Collection. *Proc. Symp. Antarct. Meteorites* **20**, 33–52.

SCHERER P. AND SCHULTZ L. (1999) Noble gases in the SNC meteorite Dar al Gani 476 (abstract). *Lunar Planet. Sci.* **30**, #1144, Lunar and Planetary Institute, Houston, Texas, USA (CD-ROM).

SMITH K. L., MILNES A. R. AND EGGLETON R. A. (1987) Weathering of basalt: Formation of iddingsite. *Clays Clay Min.* **35**, 418–428.

STEELE I. M. AND SMITH J. V. (1982) Petrography and mineralogy of two basalts and olivine-pyroxene-spinel fragments in achondrite EETA79001. *Proc. Lunar Planet. Sci. Conf.* **13th**, *J. Geophys. Res.* **87 (Suppl.)**, A375–A384.

STOLPER E. (1977) Experimental petrology of eucritic meteorites. *Geochim. Cosmochim. Acta* **41**, 587–611.

STOLPER E. AND MCSWEEN H. Y., JR. (1979) Petrology and origin of the shergottite meteorites. *Geochim. Cosmochim. Acta* **43**, 1475–1498.

TREIMAN A. H., MCKAY G. A., BOGARD D. D., WANG M-S., LIPSCHUTZ M. E., MITTLEFEHLDT D. W., KELLER L., LINDSTROM M. M. AND GARRISON D. (1994) Comparison of the LEW 88516 and ALHA77005 martian meteorites: Similar but distinct. *Meteoritics* **29**, 581–592.

WADHWA M., MCSWEEN H. Y., JR. AND CROZAZ G. (1994) Petrogenesis of shergottite meteorites inferred from minor and trace element microdistributions. *Geochim. Cosmochim. Acta* **58**, 4213–4229.

WADHWA M., CROZAZ G., LENTZ R. AND MCSWEEN H. Y., JR. (1999) Trace-element distributions in the new Saharan martian meteorite Dar al Gani 476: Another bridge between lherzolitic and basaltic shergottites (abstract). *Meteorit. Planet. Sci.* **34 (Suppl.)**, A117–A118.

WIENS R. C. (1988) Noble gases released by vacuum crushing of EETA79001 glass. *Earth Planet. Sci. Lett.* **91**, 55–65.

WOODEN J. L., SHIIH C-Y., NYQUIST L. E., BANSAL B. M., WIESMANN H. AND MCKAY G. A. (1982) Rb-Sr and Sm-Nd isotopic constraints on the origin of EETA79001 (abstract). *Lunar Planet. Sci.* **13**, 879–880.

YANAI K. AND KOJIMA H. (1981) *Photographic Catalog of the Selected Antarctic Meteorites*. National Institute of Polar Research, Tokyo, Japan. 60 pp.

ZIPFEL J. (1998) Dar al Gani 400: Chemistry and petrology of the largest lunar meteorite (abstract). *Meteorit. Planet. Sci.* **33 (Suppl.)**, A171.

ZIPFEL J. (1999) Pyroxene and olivine in basaltic shergottite Dar al Gani 476 (abstract). *Meteorit. Planet. Sci.* **34 (Suppl.)**, A123–A124.

ZIPFEL J., SPETTEL B., PALME H. AND DREIBUS G. (1999) Petrology and chemistry of Dar al Gani 476: A new basaltic shergottite (abstract). *Lunar Planet. Sci.* **30**, #1206, Lunar and Planetary Institute, Houston, Texas, USA (CD-ROM).

ZIPFEL J., SCHERER P., SPETTEL B., DREIBUS G. AND SCHULTZ L. (2000) Petrology and chemistry of the new shergottite Dar al Gani 476. *Meteorit. Planet. Sci.* **35**, 95–106.